PROCEEDINGS OF SCIENCE

Large-scale anisotropies above 0.03 EeV measured by the Pierre Auger Observatory

Esteban Roulet[*a] **for the Pierre Auger Collaboration**[b†]
[a]*Centro Atómico Bariloche, Comisión Nacional de Energía Atómica*
Consejo Nacional de Investigaciones Científicas y Técnicas (CONICET)
Av. Bustillo 9500, R8402AGP, Bariloche, Argentina
[b]*Observatorio Pierre Auger, Av. San Martín Norte 304, 5613 Malargüe, Argentina*
E-mail: auger_spokespersons@fnal.gov
Full author list: http://www.auger.org/archive/authors_icrc_2019.html

We present analyses of the large-scale anisotropies observed by the Pierre Auger Observatory over more than three decades in energy, considering data since 1 January 2004 up to 31 August 2018. For $E \geq 4$ EeV, for which the array with 1500 m separation between detectors is fully efficient, we obtain the dipolar and quadrupolar amplitudes through a combined Fourier analysis of the distribution of events in right ascension and azimuth. A dipolar modulation with an amplitude $d = 6.6^{+1.2}_{-0.8}\%$ and pointing $\sim 125^\circ$ away from the Galactic center is observed above 8 EeV. The dipole amplitude shows an indication of an increase with energy above 4 EeV and the quadrupolar components turn out to be not significant. Astrophysical scenarios that could account for these results are briefly discussed. We also extend the study of the equatorial component of the dipolar modulation down to ~ 0.03 EeV. In the regime in which the efficiencies are small, we use the East-West method, which is largely insensitive to systematic effects. Finally, for the lowest energies we use the data from a subarray with 750 m separation between detectors. The results suggest a change in the phase of the equatorial dipole from values pointing close to the right ascension of the Galactic center below EeV energies towards values indicative of an extragalactic origin for the dipolar anisotropy above a few EeV.

36th International Cosmic Ray Conference — ICRC2019
24 July – 1 August, 2019
Madison, Wisconsin, USA

*Speaker.
†for collaboration list see PoS(ICRC2019)1177

PoS(ICRC2019)408

1. Introduction

The origin of ultrahigh energy cosmic rays is still one of the important open problems in high-energy astrophysics. Besides the information that can be obtained from the observation of the spectrum and the composition of the cosmic rays (CRs), the other crucial handle for this is the study of the anisotropies in their arrival direction distribution. Being charged particles, their deflections in the Galactic and extragalactic magnetic fields make the identification of their sources very challenging. Moreover, the suggested trend towards a heavier composition that is inferred to happen above few EeV leads one to expect that only at the highest observed energies may the average deflections of the CRs from an extragalactic source be smaller than a few tens of degrees. On the other hand, anisotropies on large angular scales, such as a dipole or a quadrupole, may be present at all CR energies. They may arise from the anisotropic distribution of the CR sources themselves, either if the CR propagation is quasi-rectilinear or diffusive. They may also result from individual extragalactic CR sources if the magnetic fields are strong enough so that the propagation is diffusive, and they could also be produced at lower energies by CRs from Galactic sources as they escape from the Galaxy.

2. The dataset

In this work, we consider data collected up to 31 August 2018 at the Pierre Auger Observatory [1]. We consider the data from the surface arrays, since having $\sim 100\%$ duty cycle they provide a significantly larger number of events than the fluorescence telescopes. Another advantage is that their associated exposure has a much simpler angular dependence. We consider the 3000 km^2 array in which the detectors are separated by 1500 m (SD1500), which is fully efficient above ~ 3 EeV for events with zenith angles $\theta \leq 60^\circ$ (vertical events) and above 4 EeV for the events with $60^\circ < \theta \leq 80^\circ$ (inclined events).[1] We also use the vertical SD1500 events in the regime below full efficiency, in which case the energy assignment is done by extrapolating the calibration curve established with events having energies above 3 EeV. At the lowest energies, and going down to 0.03 EeV, it proves convenient to use the smaller 23 km^2 sub-array with 750 m separation between detectors (SD750), which is fully efficient down to ~ 0.3 EeV for events with $\theta \leq 55^\circ$. For the SD1500 array, we consider events since 1 January 2004, amounting to a total exposure of 92,500 km^2 yr sr for $\theta \leq 80^\circ$ (and a relaxed trigger), and 60,700 km^2 yr sr for $\theta \leq 60^\circ$. For the SD750 array, we use the events since 1 January 2012, amounting to a total exposure of 234 km^2 yr sr. We split the data above ~ 0.03 EeV into 11 energy bins, with the energies defining the boundaries scaling by factors of two, i.e., $E_n = 2^n$ EeV, with $n = -5, -4, ..., 4, 5$, and with the highest energy bin corresponding to $E \geq 32$ EeV. We also report the results for the cumulative bin $E \geq 8$ EeV that was considered in previous works. The analyses presented here update those performed above full efficiency of the SD1500 in Refs. [2, 3, 4], and extend those in right ascension down to 0.03 EeV [5] (see also [6, 7, 8]).

[1] For energies above 4 EeV, we consider a relaxed trigger in which we allow for the possibility that one of the stations around the one with the highest signal may not be working. Below 4 EeV we do not include the inclined events and require that all six surrounding stations be functioning.

3. Systematic effects

The main difficulty that one has to face in order to determine the large-scale anisotropies is that, besides requiring the detection of a large number of events given the small expected amplitudes, it is also necessary that all possible sources of systematic effects that could lead to spurious signals be well under control and accounted for. The main sources for these systematic effects are:

- The exposure of the array is not perfectly uniform over time, due to the initial detector deployment period, sporadic down-times, etc. To account for this requires one to monitor the number of active detector units (each one corresponding to an hexagon of adjacent working detectors) at every minute and include this information in a weight that is assigned to each event in the Fourier analysis being performed.

- The variation of the atmospheric conditions, such as changes in the air density and pressure, affect the development of the air showers, changing respectively the Molière radius and the total column density traversed [9]. In particular, given the fact that the CR energy is estimated from the reconstructed value of the signal at 1 km from the shower core (450 m for the SD750 array), under hot weather conditions the lower air densities tend to lead to an increased lateral spread of the showers and hence to an overestimate of the primary CR energy. If not accounted for, this would lead to spurious daily and seasonal variations of the CR flux above a given energy threshold. This effect has been studied in detail, and it is taken into account in the energy assignment of the vertical events (the air showers of inclined events are dominated by the muonic component, whose dependence on atmospheric conditions is negligible at these energies).

- The geomagnetic field also affects the shower development, in particular by increasing the lateral spread of the muonic component. This spread is larger for showers that are more perpendicular to the magnetic field direction, what induces spurious dipolar and quadrupolar components in the azimuthal distribution of the events. This is corrected in the energy assignment of the vertical events following Ref. [10] (for inclined showers, the geomagnetic field effects are already accounted for in their standard energy assignment).

- The array has a slight tilt, of about $\theta_t \simeq 0.2^\circ$ on average, towards the SE direction ($\phi_t \simeq -30^\circ$ with respect to the East direction). This tilt could induce a slight net excess of events from the South, which we correct for through the weights introduced for each event in the Fourier analysis.

4. Method

Above the full trigger efficiency of the array, we perform a weighted Fourier analysis in right-ascension and azimuth ($x = \alpha$ or ϕ respectively). The Fourier components are

$$a_k^x = \frac{2}{\mathcal{N}} \sum w_i \cos(k x_i) \ , \ b_k^x = \frac{2}{\mathcal{N}} \sum w_i \sin(k x_i), \tag{4.1}$$

where the sums run over all events with $i = 1, N$, the normalization factor is $\mathscr{N} = \sum w_i$, k is the order of the harmonic (e.g., $k = 1$ for the dipolar modulation), and the weights are obtained from

$$w_i^{-1} = \Delta N_{\rm hex}(\alpha_i^0)\,[1 + \tan\theta_{\rm t}\tan\theta_i\cos(\phi_i - \phi_{\rm t})]\,, \tag{4.2}$$

with $\Delta N_{\rm hex}(\alpha_i^0)$ being the normalized differential exposure of the array as a function of the right-ascension of the zenith of the observatory at the time the i-th event is recorded. The amplitudes and phases of the harmonics are then obtained as $r_k^x = \sqrt{(a_k^x)^2 + (b_k^x)^2}$ and $\varphi_k^x = \text{atan}(b_k^x/a_k^x)/k$.

Below full trigger efficiency there are other systematic effects entering into play. Although the efficiency does not depend directly on the right ascension, there is an interplay between the atmospheric effects, which for any given event modify the signals expected at the different stations, and the trigger probability which ultimately depends on those signals. We have found that for the SD1500 array, even accounting for these effects, there are indications of the presence of surviving systematic effects below 2 EeV, as is apparent in the non-negligible amplitudes that remain at the anti-sidereal frequency which suggests that a comparable spurious amplitude could also be present at the sidereal frequency. On the other hand, we have checked that above 2 EeV the first-harmonic amplitudes at both the solar and anti-sidereal frequencies are compatible with being due to statistical fluctuations. Below 2 EeV, one can use instead the East-West (EW) method [11], which relies on the fact that the exposure and atmospheric systematic effects are equal for events coming from the eastern or western hemispheres. This implies that their difference provides a clean measurement of the derivative of the modulation in right ascension, from which the actual modulation can be safely recovered although with a larger uncertainty. For events with energies smaller than 0.25 EeV, it actually turns out to be convenient to use the data from the SD750 array, which although being smaller is more efficient at low energies. Since the SD750 array is not fully efficient below 0.3 EeV, we just use the EW method in this case, extending the analysis down to 0.03 EeV. We note that for the Fourier analysis in right ascension the effect of the tilt of the array and of the geomagnetic corrections are not relevant (they only affect the analysis in azimuth), and hence these corrections are not implemented for the SD750 array.

The computation of the North-South component of the dipole d_z requires the knowledge of the azimuthal modulation of the rates. However, due to the geometry of the surface array layout the trigger efficiency depends on the azimuth angle, and combined with the zenith dependence of the efficiency the exposure ends up having a non-trivial dependence on declination. Moreover, the geomagnetic effects (and also those of the tilt of the array) depend on the azimuth angle, and hence their interplay with the trigger efficiency represents an additional source of systematic effects when one attempts to recover the North-South dipole component (as well as the quadrupole components) in the regime in which there is no full efficiency. We hence restrict the analysis below 4 EeV to the study of the equatorial dipole component $\vec{d}_\perp$, whose amplitude is related to that of the first harmonic in right ascension via $d_\perp \simeq r_1^\alpha/\langle\cos\delta\rangle$, with $\langle\cos\delta\rangle$ being the average cosine of the declination of the events, and whose phase α_d coincides with the phase φ_1^α.

5. Results

Table 1 contains the values for the dipolar components in the different energy bins above 4 EeV. These values are obtained under the assumption that the higher multipoles are negligible. The most

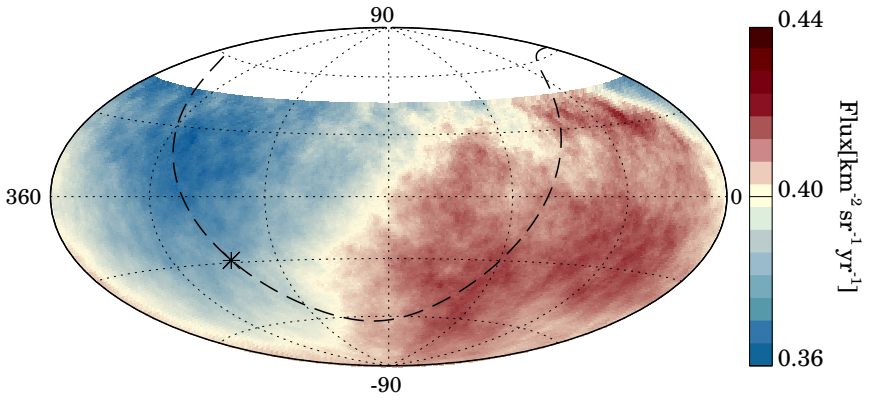

Figure 1: Map in Equatorial coordinates of the CR flux above 8 EeV, averaged on top-hat windows of 45° radius. The location of the Galactic plane is shown with a dashed line, and the Galactic center is indicated with a star.

significant result is the right ascension modulation in the cumulative bin above 8 EeV that was considered in [3], which now gives $d_\perp = 0.060^{+0.010}_{-0.009}$. The overall distribution of the flux in this bin, averaged on top-hat windows of 45°, is displayed in Fig. 1, showing a clear dipolar pattern. The total dipole amplitude in this bin is $d = 0.066^{+0.012}_{-0.008}$, and it points $\sim 125°$ away from the direction of the Galactic centre (shown with an asterisk), indicating that this anisotropy has an extragalactic origin. Considering the four energy bins above 4 EeV, a growth of the dipole amplitude with increasing energy is found, which is approximately reproduced with the expression $d = d_{10}(E/10\,\mathrm{EeV})^\beta$, with $d_{10} = 0.051 \pm 0.007$ and $\beta = 0.96 \pm 0.16$. A fit with an energy-independent dipole amplitude ($\beta = 0$) is disfavored at the level of 5.1σ by a likelihood ratio test. These results are shown in Fig. 2, where they are also compared to the predictions from Ref. [12] for scenarios of extragalactic sources with a mixed CR composition compatible with that inferred by Auger, having a density 10^{-4} Mpc^{-3} and being sampled either form an isotropic distribution or according to the distribution of galaxies in the 2MRS catalog. The direction of the dipolar anisotropy in the different bins is displayed in Fig. 3, in which the contours of equal probability per unit solid angle, marginalized over the dipole amplitude, that contain the 68%CL range are displayed. In all cases, it turns out to be not

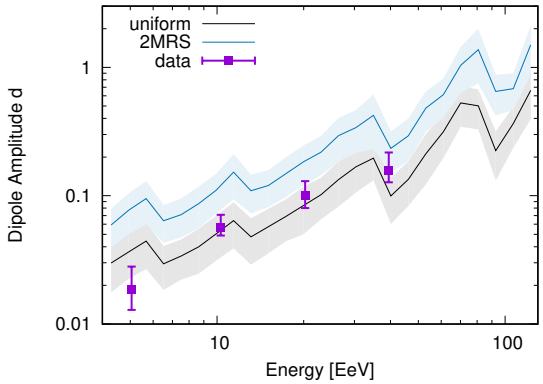

Figure 2: Energy dependence of the dipolar amplitude measured above 4 EeV. Also shown are the predictions from scenarios [12] with extragalactic sources.

Table 1: Dipole reconstruction for $E \geq 4$ EeV. Shown are the number of events in each bin N, the Equatorial amplitude $d_\perp$, the one along the rotation axis of the Earth d_z, and the total 3D amplitude d, as well as the dipole direction (α_d, δ_d).

Energy [EeV] interval	median	N	$d_\perp$	d_z	d	α_d [°]	δ_d [°]
4 - 8	5.0	88,325	$0.010^{+0.007}_{-0.004}$	-0.016 ± 0.009	$0.019^{+0.009}_{-0.006}$	69 ± 46	-57^{+24}_{-20}
≥ 8	11.5	36,928	$0.060^{+0.010}_{-0.009}$	-0.028 ± 0.014	$0.066^{+0.012}_{-0.008}$	98 ± 9	-25 ± 11
8 - 16	10.3	27,271	$0.056^{+0.012}_{-0.010}$	-0.011 ± 0.016	$0.057^{+0.014}_{-0.008}$	97 ± 12	-11 ± 16
16 - 32	20.2	7,664	$0.075^{+0.023}_{-0.018}$	-0.07 ± 0.03	$0.10^{+0.03}_{-0.02}$	80 ± 17	-44 ± 14
≥ 32	39.5	1,993	$0.13^{+0.05}_{-0.03}$	-0.09 ± 0.06	$0.16^{+0.06}_{-0.03}$	152 ± 19	-34^{+19}_{-20}

Table 2: Dipole and quadrupole components in the two energy bins. The x axis is in the direction $\alpha = 0°$.

Energy [EeV]	d_i	Q_{ij}
4 - 8	$d_x = -0.001 \pm 0.008$	$Q_{zz} = -0.003 \pm 0.039$
	$d_y = 0.008 \pm 0.008$	$Q_{xx} - Q_{yy} = -0.004 \pm 0.028$
	$d_z = -0.014 \pm 0.022$	$Q_{xy} = 0.006 \pm 0.014$
		$Q_{xz} = -0.008 \pm 0.018$
		$Q_{yz} = -0.005 \pm 0.018$
≥ 8	$d_x = -0.004 \pm 0.012$	$Q_{zz} = 0.032 \pm 0.061$
	$d_y = 0.054 \pm 0.012$	$Q_{xx} - Q_{yy} = 0.077 \pm 0.048$
	$d_z = -0.011 \pm 0.035$	$Q_{xy} = 0.038 \pm 0.024$
		$Q_{xz} = 0.015 \pm 0.029$
		$Q_{yz} = -0.016 \pm 0.029$

very different from the direction of the outer Galactic spiral arm, at Galactic coordinates $b = 0°$ and $\ell \simeq -100°$. The direction towards the flux-weighted dipole of the 2MRS galaxy distribution, which is dominated by the contribution from galaxies closer than ~ 100 Mpc, is also indicated. In this respect, it is important to keep in mind that the CR deflections induced by the Galactic magnetic field would have the effect of changing the direction of an extragalactic dipolar distribution when it is observed from the Earth, tending to align it closer to the directions towards the spiral arms, as shown in Fig. 4 for different illustrative values of the CR rigidities. These deflections also tend to reduce the resulting dipole amplitude, as indicated with the color code.

Allowing for the presence of a quadrupole, we report the reconstructed dipolar and quadrupolar components of the flux in the bins [4, 8] EeV and $E \geq 8$ EeV in Table 2, obtained as done in [2]. The five independent quadrupolar components turn out to be not significant in any of the energy bins, and hence the resulting dipolar components are consistent with those obtained ignoring the quadrupoles.

The results for the equatorial dipole component $d_\perp$, for all the bins down to $E \simeq 0.03$ EeV, are compiled in Table 3 and plotted in Fig. 5. For the bins in which the measured amplitude is smaller than the value $d_\perp^{99}$ within which 99% of the simulations with isotropic distributions of the same number of events would fall, we also report the resulting 99% CL upper bound on the

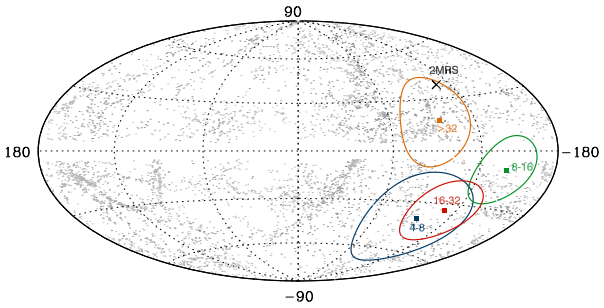

Figure 3: Reconstructed dipole direction in different energy bins, in Galactic coordinates. Dots indicate the 2MRS galaxies within 100 Mpc and the cross is the direction towards the flux weighted dipole.

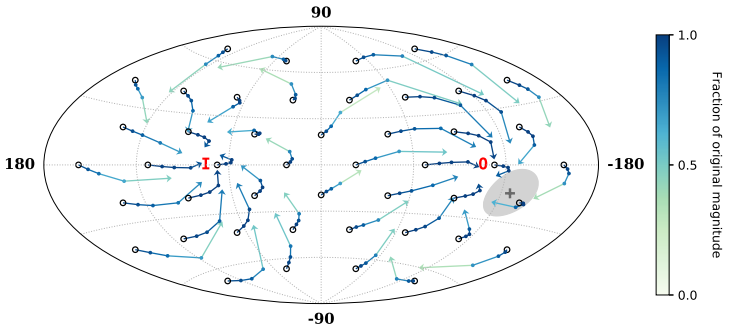

Figure 4: Map in Galactic coordinates illustrating the changes induced by the Galactic magnetic field upon an extragalactic dipolar CR distribution. Circles represent the original dipole direction outside the Galaxy and the different points along the arrows show the directions that would be observed from Earth for $E/Z =$ 32, 16, 8 and 4 EeV. The color code indicates the factor by which the observed amplitude gets reduced. The gray ellipse indicates the direction of the reconstructed dipole for $E \geq 8$ EeV.

amplitude that is inferred from the observations. One can appreciate that the measured amplitudes tend to increase with energy, from values typically smaller than about 1% below 1 EeV to values above 6% above 10 EeV. Below 1 EeV the phases in most of the bins point near the Galactic center direction, at $\alpha_{\rm GC} \simeq -94^\circ$, although none of the determined amplitudes are significant. We note that the values obtained at few PeV energies by the IceCube, IceTop and KASCADE-Grande experiments [13, 14, 15], included in the figure, also point near the Galactic center direction.

This would suggest that the transition between a predominantly Galactic and an extragalactic origin for the dipolar anisotropies is taking place somewhere between 1 and few EeV. Further studies of the large-scale anisotropies in this energy regime will help to better characterize this transition.

References

[1] A. Aab et al. (Pierre Auger Collaboration), Nucl. Instrum. Meth. A **798** (2015) 172

[2] A. Aab et al. (Pierre Auger Collaboration), Astrophys. J. 802 (2015) 111

[3] A. Aab et al. (Pierre Auger Collaboration), Science 357 (2017) 1266

[4] A. Aab et al. (Pierre Auger Collaboration), Astrophys. J. 868 (2018) 4

[5] A. Aab et al. (Pierre Auger Collaboration), in preparation

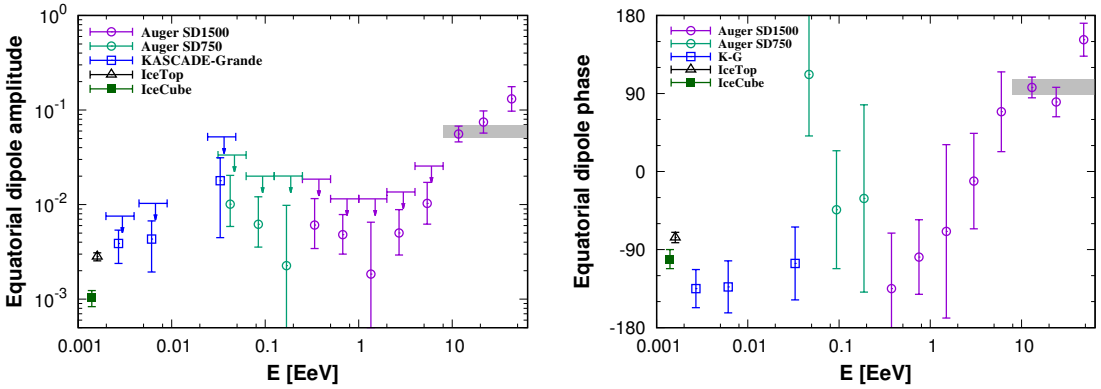

Figure 5: Amplitude (left panel) and phase (right panel) of the equatorial dipole amplitude determined in the different bins. Also shown are the low-energy results from IceCube, IceTop and KASCADE-Grande [13, 14, 15]. For the bins in which $d_\perp < d_\perp^{99}$, also the upper-limit $d_\perp^{\rm UL}$ is indicated with an arrow.

	E [EeV]	N	$d_\perp$	$\alpha_d[^\circ]$	$P(\geq d_\perp)$	$d_\perp^{99}$	$d_\perp^{\rm UL}$
East-West	0.03125 - 0.0625	432,155	$0.010^{+0.010}_{-0.004}$	112 ± 71	0.54	0.028	0.033
(SD750)	0.0625 - 0.125	924,856	$0.006^{+0.006}_{-0.003}$	-44 ± 68	0.50	0.016	0.020
	0.125 - 0.25	488,752	$0.002^{+0.008}_{-0.002}$	-31 ± 108	0.94	0.019	0.020
East-West	0.25 - 0.5	770,316	$0.006^{+0.005}_{-0.003}$	-135 ± 64	0.45	0.015	0.018
(SD1500)	0.5 - 1.0	2,388,467	$0.005^{+0.003}_{-0.002}$	-99 ± 43	0.20	0.008	0.011
	1 - 2	1,243,103	$0.0018^{+0.0047}_{-0.0002}$	-69 ± 100	0.87	0.011	0.011
Fourier	2 - 4	283,074	$0.005^{+0.004}_{-0.002}$	-11 ± 55	0.34	0.010	0.014
(SD1500)	4 - 8	88,325	$0.010^{+0.007}_{-0.004}$	69 ± 46	0.23	0.018	0.026
	8 - 16	27,271	$0.056^{+0.012}_{-0.010}$	97 ± 12	2.3×10^{-6}	0.033	–
	16 - 32	7,664	$0.075^{+0.023}_{-0.018}$	80 ± 17	1.5×10^{-3}	0.063	–
	≥ 32	1,993	$0.13^{+0.05}_{-0.03}$	152 ± 19	5.3×10^{-3}	0.12	–
	≥ 8	36,928	$0.060^{+0.010}_{-0.009}$	98 ± 9	1.4×10^{-9}	0.028	–

Table 3: Equatorial dipole reconstruction in different energy bins. Indicated are the number of events, amplitude and phase of $d_\perp$, probability to get a larger amplitude from fluctuations of an isotropic distribution, value within which 99% of the isotropic simulations fall and 99% CL upper limit on the amplitude.

[6] P. Abreu et al. (Pierre Auger Collaboration), Astrophys. J. Lett. 762 (2013) L13
[7] I. Sidelnik for the Pierre Auger Collaboration, Proceeding of the 33rd ICRC, arXiv:1307.5059
[8] I. Al Samarai for the Pierre Auger Collaboration, PoS ICRC2015 (2016) 372
[9] A. Aab et al. (Pierre Auger Collaboration), JINST 12 (2017) P02006
[10] P. Abreu et al. (Pierre Auger Collaboration), JCAP 11 (2011) 022
[11] R. Bonino et al., *Astrophys. J.* 738 (2011) 67
[12] D. Harari, S. Mollerach and E. Roulet, Phys. Rev. D 92 (2015) 063014
[13] R. Abbasi et al. (IceCube Collaboration), Astrophys. J. 746 (2012) 33
[14] M.G. Aartsen et al. (IceCube Collaboration), Astrophys. J. 826 (2016) 220
[15] A. Chiavassa et al. (KASCADE-Grande Collaboration), Nucl. Part. Phys. Proc. 279 (2016) 56